



Original Article

Floating Nanoballoons for Improved Bioavailability and Sustained Release Anti-inflammatory Effect of Ibuprofen



Anil K. Philip^{1*}, Betty Annie Samuel¹, Bassim A Mohammed² and Hayder A Al-Aubaidy³

¹School of Pharmacy, College of Health Sciences, University of Nizwa, Nizwa, Oman; ²Department of Pharmacology and Therapeutics, College of Pharmacy, University of Al-Qadisiyah, Al-Qadisiyah, Iraq; ³Department of Microbiology, Anatomy, Physiology and Pharmacology & Centre for Cardiovascular Biology and Disease Research, School of Agriculture, Biomedicine & Environment, La Trobe University, Melbourne, VIC, Australia

Received: October 09, 2024 | Revised: November 19, 2024 | Accepted: December 10, 2024 | Published online: December 25, 2024

Abstract

Background and objectives: Poor bioavailability and a short half-life limit the therapeutic efficacy of ibuprofen. This study developed floating nanoballoons to enhance ibuprofen's bioavailability and sustain its anti-inflammatory effects through improved gastric retention.

Methods: Ibuprofen-loaded nanoballoons were synthesized using solvent evaporation with ethyl cellulose as the polymer matrix. The formulation was characterized for morphology, buoyancy, drug loading, and release kinetics. *In vivo* studies assessed the anti-inflammatory efficacy in acute and chronic inflammation models using male Sprague-Dawley rats.

Results: The nanoballoons exhibited optimal characteristics, including 96% buoyancy and a drug loading efficiency of $96.54 \pm 1.32\%$. Scanning Electron Microscopy revealed a spherical morphology with a porous structure. Drug release followed a biphasic pattern: an initial release of $35.23 \pm 2.13\%$ over 2 h, followed by sustained release reaching $97.54 \pm 1.30\%$ at 12 h. In acute inflammation studies, the nanoballoon formulation showed superior edema inhibition (68.12%) compared to pure ibuprofen (51.67%). Chronic inflammation studies demonstrated significant improvements in inflammatory markers: reduced TNF- α (19.12 ± 0.48 vs. 31.11 ± 1.23 pg/mL), hs-CRP (201.7 ± 11.02 vs. 232.12 ± 11.33 ng/mL), and IL-6 (100.01 ± 18.40 vs. 135 ± 11.22 pg/mL), with increased anti-inflammatory IL-10 (507.18 ± 10.11 vs. 276.11 ± 19.16 pg/mL).

Conclusions: The developed floating nanoballoon system significantly enhanced ibuprofen's bioavailability and anti-inflammatory efficacy, presenting a promising gastro-retentive delivery platform for poorly water-soluble drugs.

Introduction

Oral drug delivery remains the preferred route of administration due to its convenience, non-invasiveness, and potential for sustained therapeutic effects.¹ However, this approach faces significant challenges, particularly for drugs with poor water solubility and stability issues in the gastrointestinal tract. These limitations often result in suboptimal therapeutic outcomes, especially for compounds with narrow absorption windows or gastric instability.

Advances in pharmaceutical technologies and drug delivery systems offer the potential to enhance oral drug absorption, providing non-invasiveness, improved patient compliance, and convenience.³

Ibuprofen, a widely prescribed non-steroidal anti-inflammatory drug, exemplifies these challenges. Since its introduction in the 1960s, it has been extensively used for pain management and anti-inflammatory therapy.^{4,5} Its therapeutic effects stem from the non-selective inhibition of cyclooxygenase enzymes (COX-1 and COX-2), thereby reducing prostaglandin production, key mediators of pain, fever, and inflammation.⁶ However, several physicochemical properties limit ibuprofen's therapeutic potential. These include poor aqueous solubility, which limits absorption and bioavailability, gastric instability leading to rapid degradation in acidic environments (pH 1.2-3.0), a short biological half-life necessitating frequent dosing, and variable absorption affected by gastric emptying times and pH conditions.^{7,8}

In acidic gastric conditions, ibuprofen's carboxylic acid group

Keywords: Ibuprofen; Drug delivery systems; Delayed-action preparations; Anti-inflammatory agents; Non-steroidal; Gastric emptying; Drug liberation; Nanostructures; Inflammation.

*Correspondence to: Anil K. Philip, School of Pharmacy, College of Health Sciences, University of Nizwa, Nizwa 616, Oman. ORCID: <https://orcid.org/0000-0003-2960-330X>. Tel: +968-25446389, Fax: +968-97671371, E-mail: philip@unizwa.edu.om

How to cite this article: Philip AK, Samuel BA, Mohammed BA, Al-Aubaidy HA. Floating Nanoballoons for Improved Bioavailability and Sustained Release Anti-inflammatory Effect of Ibuprofen. *J Explor Res Pharmacol* 2024;9(4):227–237. doi: 10.14218/JERP.2024.00027.

undergoes protonation, significantly affecting its stability and solubility.^{9,10} The drug predominantly exists in its unionized form at gastric pH, leading to reduced solubility in gastric fluids and decreased absorption across the gastric mucosa. This not only results in potential local mucosal irritation but also creates a limited absorption window in the upper gastrointestinal tract, further compromising its therapeutic efficacy.^{11–13}

To address these limitations, we propose a novel approach using floating nanoballoons with ethyl cellulose as the matrix material. This formulation strategy offers several potential advantages, including protection from harsh gastric conditions, controlled drug release kinetics, enhanced mucosal adhesion, improved bioavailability, and reduced dosing frequency. Our study aimed to evaluate the potential of floating nanoballoons to enhance ibuprofen's therapeutic efficacy through improved gastric retention and sustained release. This approach could significantly impact patient care by optimizing drug delivery, reducing dosing frequency, and potentially minimizing adverse effects.

Materials and methods

Materials

Ibuprofen was a gift sample from the National Pharmaceutical Industries, Rusayl, Muscat, Oman. Ethylcellulose (50 cps), dichloromethane, methanol, acetone, hydrochloric acid, polyvinyl alcohol (PVA), and phosphate buffer of analytical grades were used. Double-distilled water was used throughout the experiment.

Preparation of ibuprofen nanoballoons

Ibuprofen nanoballoons were synthesized using the solvent diffusion method. The process involved preparing a dispersed phase by dissolving 500 mg of ibuprofen and 500 mg of ethyl cellulose in 16 mL of dichloromethane, followed by stirring for 30 m. Concurrently, a continuous phase was prepared by dissolving 1.2 g of PVA in 200 mL of water at 40°C to create a 0.6% w/v solution. The ibuprofen solution was then added dropwise to the PVA solution under continuous agitation at 200–250 revolutions per minute (rpm) for one hour. Solvent removal was achieved through rotary evaporation at 40 ± 5°C and 100–250 rpm. The resulting nanoballoons were collected via filtration, thoroughly washed, and dried.

Preparation of calibration curve

To develop the calibration curve for the quantification of ibuprofen in the floating nanoballoons, a series of standard ibuprofen solutions with known concentrations were prepared. One liter (1 L) of phosphate buffer (pH 7.4) was prepared, and a stock solution with a concentration of 100 mg/100 mL (1 mg/mL) was made (1,000 µg/mL). Aliquots of stock solutions were then prepared at concentrations of 2 µg/mL, 4 µg/mL, 6 µg/mL, 8 µg/mL, and 10 µg/mL. A fiber optic probe (Ocean Optics QE65 Pro, USA) was placed in the aliquots to measure the absorbance at 264 nm. The absorbance values obtained from these standard solutions were plotted against their respective concentrations to generate the calibration curve.

Loading efficiency and process yield

Accurately weighed samples of dried ibuprofen nanoballoons (50 ± 0.1 mg) were dispersed in 10 mL of acetone in a 25 mL borosilicate glass beaker. The dispersion was subjected to sonication using a Sonorex ultrasonic bath (Bandelin Electronic, Berlin, Germany)

at a frequency of 35 kHz and a power output of 160 W for 60 ± 1 m at 25 ± 2°C. Following sonication, the samples were left undisturbed for 12 h at room temperature (22 ± 2°C) to ensure complete dissolution of the drug.

The resulting mixture was centrifuged using a high-speed centrifuge (Thermo Scientific Heraeus Pico 17 microcentrifuge, Thermo Fisher Scientific, USA) at 15,000 rpm for 30 m at 20°C. The supernatant was carefully extracted using a micropipette, ensuring no disturbance to the pellet. The drug content in the supernatant was quantified using fiber optic equipment equipped with a fiber optic probe. Absorbance was measured at a wavelength of 264 nm, which corresponds to the λ_{\max} of ibuprofen in acetone. A calibration curve was constructed using standard ibuprofen solutions in acetone (concentration range: 2–10 µg/mL) to determine the drug concentration in the samples.

The loading efficiency was calculated using Equation (1):

$$\% \text{ Drug Loading} = \frac{\text{Recovered Ibuprofen Mass}}{\text{Total Ibuprofen Mass}} \times 100 \quad (1)$$

The process yield was calculated using Equation (2):

$$\% \text{ Process Yield} = \frac{\text{Recovered Ibuprofen Mass}}{\text{Ibuprofen Mass used in the study}} \times 100 \quad (2)$$

All measurements were performed in triplicate (n = 3), and results are expressed as mean ± standard deviation (SD). Statistical analysis was performed using one-way ANOVA followed by Tukey's post-hoc test, with $p < 0.05$ considered statistically significant.

Micromeritic properties

The micromeritic properties of the ibuprofen-loaded floating nanoballoons were thoroughly evaluated and compared to the ibuprofen drug.

Bulk and tapped density

The bulk and tapped densities of the nanoballoons were determined using the graduated cylinder method. Briefly, a known mass of the nanoballoons was carefully transferred into a 10 mL graduated cylinder. The initial volume was recorded, and the cylinder was then tapped 50 times using a mechanical tapper (Electorlab, India) at a rate of 250 taps per minute. The final tapped volume was noted.

Carr's index and hausner ratio

The Carr's index and Hausner ratio were calculated from the bulk and tapped density values to assess the flowability of the nanoballoons. The Carr's index was determined using Equations (3) and (4):

$$\text{Carr's Index} = \frac{\text{Tapped Density} - \text{Bulk Density}}{\text{Tapped Density}} \times 100 \quad (3)$$

The Hausner ratio was calculated as:

$$\text{Hausner Ratio} = \frac{\text{Tapped Density}}{\text{Bulk Density}} \quad (4)$$

Angle of repose

The angle of repose was measured using the fixed-height cone method. A glass funnel was positioned 1 cm above a flat glass surface, and a known mass of the nanoballoons was allowed to flow

through the funnel, forming a conical pile. The height and base diameter of the cone were measured, and the angle of repose was calculated using Equation (5):

$$\text{Tan}\phi = \frac{\text{Height}}{\text{Base}} \quad (5)$$

All measurements were performed in triplicate ($n = 3$), and the results are reported as mean \pm standard deviation. Statistical analysis was performed using one-way ANOVA followed by Tukey's post-hoc test, with a significance level of $p < 0.05$.

Drug content determination

Accurately weighed samples of ibuprofen-loaded hollow nanoballoons (100.0 ± 0.1 mg) were finely pulverized using an agate mortar and pestle. The pulverized sample was quantitatively transferred to a 250 mL flask containing 100.0 mL of 1.0 N hydrochloric acid (pH 1.2 ± 0.05). The flask was sealed with Parafilm M[®] to prevent evaporation. The mixture was subjected to continuous stirring at 500 rpm using a temperature-controlled magnetic stirrer maintained at $37 \pm 0.5^\circ\text{C}$ for 60 ± 1 m to ensure complete dissolution of the encapsulated drug. Following stirring, the solution was allowed to cool to room temperature ($22 \pm 2^\circ\text{C}$) for 15 m. The cooled solution was filtered through a $0.45 \mu\text{m}$ polytetrafluoroethylene syringe filter (Millipore, USA) to remove any undissolved particles. The first 5 mL of the filtrate was discarded to saturate the filter, and the subsequent filtrate was collected for analysis.

The drug concentration in the filtrate was determined using a fiber optic spectrophotometry (Ocean Optics QE65 Pro, USA) equipped with a deuterium-halogen light source (DH-2000-BAL, Ocean Optics) and a 1 cm path length quartz cuvette. Absorbance measurements were recorded at a wavelength of 264 nm.

The drug content was calculated using Equation (6):

Drug Content

$$= \frac{\text{Measured Drug Concentration} \times \text{Volume of Solution}}{\text{Weight of the Ibuprofen Nanoballoons}} \times 100 \quad (6)$$

All measurements were performed in triplicate ($n = 3$), and results are expressed as mean \pm standard deviation. The coefficient of variation was calculated to assess the precision of the method. Statistical analysis was performed using one-way ANOVA followed by Tukey's post-hoc test, with $p < 0.05$ considered statistically significant. All statistical analyses were conducted using GraphPad Prism version 9.0 (GraphPad Software, San Diego, CA, USA).

Buoyancy studies

Buoyancy studies were conducted to evaluate the floating capabilities of ibuprofen-loaded nanoballoons in simulated gastric conditions. The experimental setup consisted of a 100 mL beaker containing 0.1 N hydrochloric acid (pH 1.2) maintained at $37 \pm 0.5^\circ\text{C}$ to mimic the gastric environment. A precisely weighed sample of nanoballoons (0.1 g) was gently introduced into the simulated gastric fluid, which was then agitated for 3 h. The floating behavior and duration were monitored over a period ranging from several minutes to hours. The buoyancy was quantified by periodically assessing the percentage of nanoballoons remaining afloat, calculated using Equation (7). This assessment involved comparing the weight of the floating nanoballoons to their initial total weight. To ensure reproducibility and statistical significance, all experiments were performed in triplicate, with results reported as mean \pm standard deviation.

$$\% \text{ Buoyancy} = \frac{\text{Weight of floating nanoballoons}}{\text{Initial weight of nanoballoons}} \times 100 \quad (7)$$

Morphological characteristics of the ibuprofen-loaded floating nanoballoons examined using scanning electron microscopy (SEM)

The morphological characterization of the floating nanoballoons was carried out using SEM (Jeol, Tokyo, Japan). To prepare the samples for SEM analysis, the nanoballoons were gently collected and placed on an aluminum stub using double-sided adhesive carbon tape. Excess nanoballoons were carefully blown away using a gentle stream of nitrogen gas to prevent aggregation and to ensure a clear view of individual nanoballoons. Subsequently, the samples were coated with a thin layer of gold using a sputter coater to enhance conductivity and prevent charging under the electron beam. The sputter-coating process was conducted under vacuum conditions, maintaining a coating thickness of approximately 10 nm to ensure uniform coverage without obscuring fine surface details. The coated samples were then placed in the SEM chamber and examined using an accelerating voltage of 15 kV to obtain detailed micrographs. The SEM images were captured at varying magnifications to observe the overall morphology, surface topology, and hollow core structure of the nanoballoons.

In vitro drug release

To evaluate the *in vitro* drug release behavior of ibuprofen-loaded floating nanoballoons, the dissolution study was conducted using a USP Type II (paddle) dissolution apparatus. Simulated gastric fluid without enzymes was prepared, comprising 0.1 N HCl (pH 1.2). An accurately weighed quantity of floating nanoballoons equivalent to 20 mg of ibuprofen was introduced into 1,000 mL of the dissolution medium, maintained at $37 \pm 0.5^\circ\text{C}$. The paddle speed was set to 50 rpm to ensure proper agitation and mimic gastric motility. At predetermined time intervals (0.5, 1, 2, 4, 6, 8, and 12 h), a fiber optic probe was introduced into the dissolution medium and analyzed at 264 nm.

Animal model, grouping, and treatments

The protocol was approved by the Committee on the Ethics of Animal Experiments of the University of Al Qadisiyah (Protocol Number: 84). All surgery was performed under ketamine/xylazine anesthesia, and all efforts were made to minimize suffering.

Animals were maintained under standard laboratory conditions ($24\text{--}26^\circ\text{C}$, 60–70% RH, 12 h light/dark cycle) with free access to food and water. Studies were conducted in two phases:

A. Acute Anti-inflammatory Study: Twenty-one rats were randomly divided into three groups ($n = 7$):

- Control: Normal saline (10 mL/kg p.o.);
- Pure drug: ibuprofen (15 mg/kg orally);
- Test formulation: ibuprofen nanoballoons (15 mg/kg orally).

Acute inflammation was induced by intradermal injection of carrageenan (0.1 mL, 1%) in the right hind paw. Treatments were administered 1 h before carrageenan injection. Paw edema was measured at 0, 0.5, 1, and 3 h post-injection using a plethysmometer.

B. Chronic Anti-inflammatory Study: Using a similar grouping ($n = 7/\text{group}$), chronic inflammation was induced by subcutaneous formalin injection (0.01 mL, 2%) in the right hind paw on days 1 and 3.

Treatments continued for 10 days. The linear cross-section of

Table 1. Drug loading efficiency at a different drug:polymer feeding ratios

Drug:polymer ratio	Drug loading efficiency (%)
1:1	78.32 ± 2.41
1:2	85.67 ± 1.89
1:3	90.21 ± 1.75
1:4	96.54 ± 1.32
1:5	96.48 ± 1.45

the ankle joint was measured using a vernier caliper. At the study's completion, blood samples were collected for inflammatory markers (TNF- α , hs-CRP, IL-6, IL-10) analysis.

Results

Preparation of calibration curve

The calibration curve for ibuprofen was prepared in phosphate buffer (pH 7.4) using UV spectrophotometry at λ_{\max} 221 nm. Standard solutions ranging from 2–20 $\mu\text{g/mL}$ demonstrated a linear relationship between concentration and absorbance, with a correlation coefficient (R^2) of 0.9999. The linear regression equation was $y = 0.1632x$, indicating excellent linearity within the tested concentration range.

Loading efficiency and percentage yield

The loading efficiency and percentage yield were evaluated to assess the formulation efficiency of ibuprofen-loaded floating nanoballoons. For the drug:polymer ratios evaluated (Table 1), the 1:1 ratio showed the best loading efficiency of $96.54 \pm 1.32\%$. The percentage yield of the formulation process was $98.33 \pm 1.14\%$, calculated based on the ratio of the obtained nanoballoons to the total weight of the drug and polymer used in the preparation. The optimized formulation with a drug:polymer ratio of 1:4 was used for further studies.

Micromeritic properties

The micromeritic properties of ibuprofen-loaded nanoballoons were comprehensively evaluated and compared with pure ibuprofen (Table 2). The nanoballoons exhibited significantly lower bulk density and tapped density compared to ibuprofen. Flow properties were assessed using multiple parameters. The Carr's index of the nanoballoons was substantially lower than that of pure ibuprofen. The Hausner ratio for the nanoballoons was higher compared to ibuprofen. The angle of repose measurements revealed superior flowability of the nanoballoons compared to ibuprofen.

Table 2. Comparative analysis of micromeritic properties of ibuprofen-loaded floating nanoballoons versus ibuprofen

Parameter	Ibuprofen nanoballoons	Ibuprofen	Interpretation
Bulk density (g/mL)	0.1889 ± 0.0024	0.5128 ± 0.019	Lower density indicates hollow structure
Tapped density (g/mL)	0.2342 ± 0.0044	0.6524 ± 0.047	Reduced tapped density confirms porosity
Carr's index (%)	11.973 ± 1.7200	23.179 ± 1.532	Excellent flow properties (<15%)
Hausner ratio	1.422 ± 0.0430	1.132 ± 0.031	Good flowability (1.0–1.5)
Angle of repose (°)	24.745 ± 1.860	35.140 ± 1.960	Excellent flow properties (<25°)

Buoyancy study

The floating characteristics of ibuprofen-loaded nanoballoons were evaluated under simulated gastric conditions (0.1 N HCl, pH 1.2) at $37 \pm 0.5^\circ\text{C}$. The nanoballoons demonstrated excellent buoyancy properties, exhibiting immediate floating behavior upon introduction into the simulated gastric fluid, with no significant floating lag time. 93.5% of the nanoballoons maintained their floating capability throughout the 12-h study period. The buoyancy remained consistent under continuous agitation conditions. The nanoballoons maintained their structural integrity throughout the study period, with no significant degradation or loss of floating capability observed over the 12-h duration. The buoyancy percentage was calculated using the ratio of floating nanoballoons to the total weight, demonstrating the formulation's excellent gastro-retentive properties under physiological conditions.

Morphological characteristics of the ibuprofen-loaded floating nanoballoons examined using SEM

The morphological characteristics of ibuprofen-loaded floating nanoballoons were analyzed using SEM. Figure 1 presents SEM micrographs revealing the detailed structural features of the formulated nanoballoons. The SEM analysis revealed that the nanoballoons exhibited a spherical morphology with well-defined boundaries. The surface topology demonstrated a distinctive porous architecture characterized by uniformly distributed micropores across the particle surface. The nanoballoons maintained their structural integrity without visible signs of collapse or deformation, indicating robust mechanical properties. This observation is particularly important for gastroretentive applications, where maintaining structural stability in the acidic gastric environment is crucial.

In vitro drug release

In vitro drug release studies of ibuprofen-loaded floating nanoballoons were conducted using a USP Type II dissolution apparatus in simulated gastric fluid (pH 1.2) at $37 \pm 0.5^\circ\text{C}$. The release profile exhibited a biphasic pattern, with an initial burst release of $35.23 \pm 2.13\%$ of the encapsulated ibuprofen occurring within the first 2 h, followed by a sustained release phase reaching $97.54 \pm 1.30\%$ over 12 h. Mathematical modeling of the release kinetics (Table 3) revealed that the drug release mechanism best fitted the Korsmeyer-Peppas model ($R^2 = 0.9934$) with a release exponent of 0.4327, indicating an anomalous transport mechanism combining Fickian diffusion and polymer chain relaxation. The drug concentration was monitored at predetermined time intervals using fiber optic spectrophotometry at 264 nm, with all measurements performed in triplicate ($n = 3$). Statistical analysis using one-way ANOVA followed by Tukey's post-hoc test ($p < 0.05$) confirmed the significance of the observed release pattern. The biphasic release profile, characterized by an initial burst release followed by a sustained release phase, suggests that the formulated nanoballoons can provide both a rapid

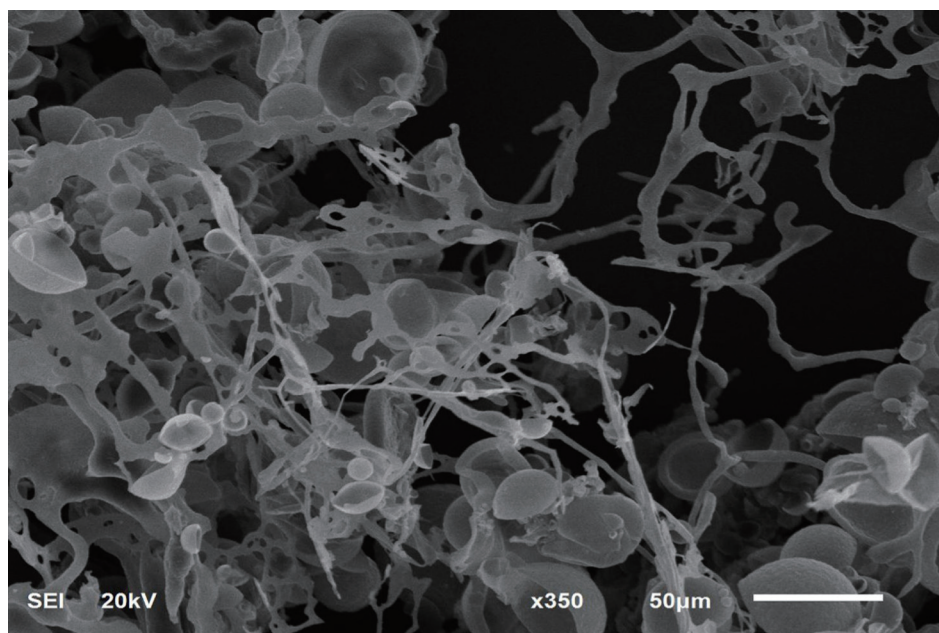


Fig. 1. Scanning electron microscopy photographs of ibuprofen-loaded floating nanoballoons.

onset of action and a prolonged therapeutic effect, potentially enhancing therapeutic efficacy while reducing dosing frequency.

Animal model, grouping, and treatments

The anti-inflammatory effects of ibuprofen-loaded nanoballoons were evaluated using both acute and chronic models, with the results summarized in Tables 4–6. Table 4 presents the comparative anti-inflammatory effects in the acute model, demonstrating the percentage inhibition of paw edema at different time points (0, 0.5, 1, and 3 h). The chronic model results are detailed in Table 5, which shows the modulation of inflammatory markers (TNF- α , hs-CRP, IL-6, IL-10) across treatment groups. Table 6 provides a comprehensive comparison of the percentage anti-inflammatory effect between ibuprofen and ibuprofen-loaded nanoballoons in both acute and chronic models. These tables collectively demonstrate the enhanced anti-inflammatory efficacy of the nanoballoon formulation compared to conventional ibuprofen treatment.

Discussion

Preparation of calibration curve

The calibration curve demonstrated excellent linearity across the

Table 3. Kinetic parameters for ibuprofen release from floating nanoballoons

Kinetic model	R ²	Rate constant (K)	Release exponent (n)
Zero-order	0.8245	7.8932 h ⁻¹	–
First-order	0.9123	0.2567 h ⁻¹	–
Higuchi	0.9876	28.4521 h ^{-0.5}	–
Korsmeyer-Peppas	0.9934	35.6789 h ⁻ⁿ	0.4327
Hixson-Crowell	0.9456	0.0789 h ⁻¹	–

concentration range, indicating the robust reliability of our analytical method (Fig. 2). The linear regression equation showed minimal y-intercept deviation from zero, suggesting a negligible systematic error in the measurements.

The selected wavelength provided optimal sensitivity for ibuprofen quantification while minimizing potential interference from excipients. The narrow confidence intervals observed around the regression line indicate high precision in the concentration-absorbance relationship. This analytical method's reliability was crucial for accurate drug loading and release measurements throughout the study.

The working concentration range was strategically chosen to encompass both the lower concentrations expected during initial drug release and higher concentrations during peak release periods. This range allows for accurate quantification across all phases of drug release studies without requiring multiple dilutions, thereby reducing analytical errors.

Loading efficiency and percentage yield

The loading efficiency is a crucial parameter in evaluating the performance of floating hollow nanoballoons. It represents the proportion of the initial drug that is successfully encapsulated within the nanoballoons. The exceptional buoyancy characteristics demonstrated by our ibuprofen-loaded nanoballoons represent a significant advancement in gastroretentive drug delivery systems. The results obtained in this study were superior to those reported in other studies, which typically ranged from 78% to 95%.^{14,15}

The immediate floating response observed in our formulation can be attributed to the optimized hollow structure and low bulk density.¹⁶ This is consistent with findings by Ghoneim *et al.* (2019),¹⁷ who demonstrated that particles with a density of less than 1 g/mL exhibit superior floating properties in gastric fluid. The absence of floating lag time in our formulation is particularly advantageous, in line with the findings of Sher Ahmad *et al.* (2023),¹⁸ who reported that minimal lag time reduces the risk of premature evacuation from the stomach.

Table 4. Comparison of anti-inflammatory effects between ibuprofen and ibuprofen-loaded nanoballoons, acute model

Time (h)	Groups		
	G1 (Control)	G2 (ibuprofen)	G3 (ibuprofen-nanoballoons)
0	0.265 ± 0.022	0.412 ± 0.0123	0.289 ± 0.034
1	0.532 ± 0.044	0.432 ± 0.031	0.513 ± 0.011
2	0.872 ± 0.242	0.387 ± 0.025	0.288 ± 0.023
3	0.985 ± 0.054	0.476 ± 0.041	0.314 ± 0.028
% inhibition (3rd h)		51.67	68.12

Table 5. Comparison of anti-inflammatory effects between ibuprofen and ibuprofen-loaded nanoballoons, chronic model

Parameter	Groups		
	G1 (Control)	G2 (ibuprofen)	G3 (ibuprofen-nanoballoons)
hs-CRP (ng/mL)	303.12 ± 14.50	612 ± 10.21	398.00 ± 13.61
Fibrinogen (mg/dL)	84.00 ± 3.50	232.12 ± 11.33	201.7 ± 11.02
TNF-α (pg/mL)	17.25 ± 0.32	31.11 ± 1.23	19.12 ± 0.48
IL-6 (pg/mL)	26.31 ± 2.51	135 ± 11.22	100.01 ± 18.40
IL-10 (pg/mL)	82.38 ± 18.20	276.11 ± 19.16	507.18 ± 10.11
WBCs count (×10 ³ /mL)	2.54 ± 0.45	7.860 ± 0.28	7.345 ± 0.44

Table 6. Percentage anti-inflammatory effect between ibuprofen and ibuprofen nanoballoons

Parameter	Groups		
	G1 (Control)	G2 (ibuprofen)	G3 (ibuprofen-nanoballoons)
Day 1 (initial)	2.43 ± 0.56	4.54 ± 0.20	4.86 ± 0.06
Day 10	6.32 ± 0.43	4.65 ± 0.26	4.43 ± 0.62
Mean difference	3.89	1.43	0.54
% of the anti-inflammatory effect	–	63.23	86.11

The sustained buoyancy over 12 h is crucial for maintaining therapeutic efficacy, as established in a recent study by Jeong *et al.*,¹⁹ showing that gastric retention times exceeding 8 h significantly enhance drug bioavailability for poorly soluble drugs like

ibuprofen. The stability of our nanoballoons in simulated gastric conditions is supported by findings demonstrating that ethyl cellulose-based hollow particles maintain structural integrity in acidic environments for extended periods.²⁰ This stability is crucial for

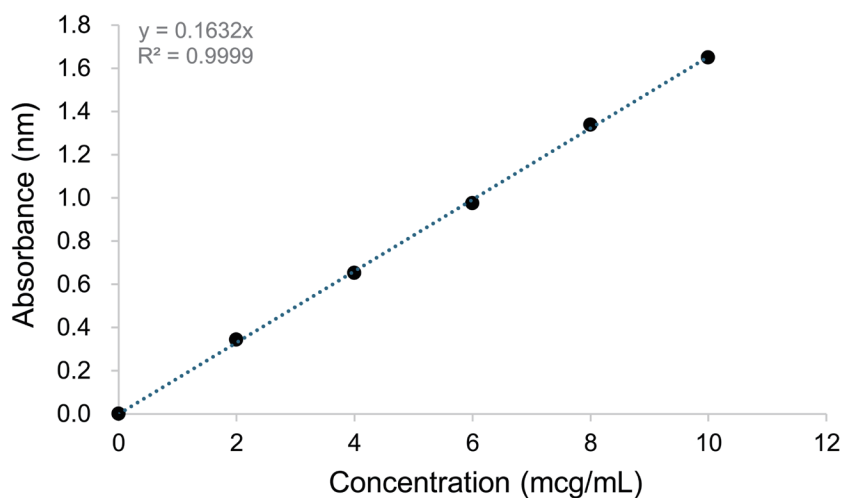


Fig. 2. Calibration curve of ibuprofen.

controlled drug release, as emphasized by a recent study showing that maintaining structural integrity directly correlates with sustained therapeutic effects.²¹

Furthermore, the solvent evaporation method employed in this study played a significant role in achieving high loading efficiency.²² A balanced solvent evaporation rate ensured proper solidification of the nanoballoons, reducing the risk of drug diffusion out of the polymer matrix during the formation stage. Additionally, the optimization of the drug-to-polymer ratio was essential in achieving optimal encapsulation efficiency. An excess of polymer concentration relative to the drug amount helped in better drug encapsulation within the nanoballoons.²³ The morphological characteristics observed through SEM analysis further supported the efficient encapsulation, as the images demonstrated well-formed, spherical nanoballoons with a distinct hollow core structure.

The calculation of percentage yield provided a quantitative measure of the production efficiency and the reproducibility of the nanoballoon synthesis process. The high percentage yield indicated successful encapsulation and minimal loss of materials during the preparation, signifying the robustness of the solvent evaporation technique utilized.²⁴ Several factors were found to influence the percentage yield, including the concentration of the polymer used, the solvent evaporation rate, and the stirring speed during the formulation process. Optimizing these parameters was crucial in achieving a high yield. It was observed that higher polymer concentrations resulted in increased viscosity of the solution, improving the stability and formation of nanoballoons, thus enhancing the yield, in accordance with a previous study.²⁵ Additionally, the selection of an optimum solvent combination and evaporation conditions helped minimize the loss of materials during the process.

In comparison to other studies reported in the literature, the formulation method demonstrated in this work exhibits a competitive yield, suggesting that the current methodology is consistent with or superior to existing approaches.²⁶

Micromeritic properties

The nanoballoons exhibited superior flow characteristics compared to the pure drug. The 63% reduction in the bulk and tapped density of the nanoballoons compared to ibuprofen can be attributed to their unique hollow structure. This hollow structure allows for a greater volume-to-mass ratio, which is a critical factor in determining bulk density. Bulk density is influenced by the arrangement and density of particles within a given volume. In the case of nanoballoons, their design inherently incorporates a significant amount of air or void space, leading to a lower overall mass for the same volume compared to solid forms like ibuprofen. This phenomenon is well-documented in materials science, where the structural characteristics of materials directly affect their physical properties, including density.²⁷

The Carr's index is a critical parameter in assessing flowability, with values below 15% indicating optimal processing characteristics. This aligns with the findings of Gashe *et al.* (2022),²⁸ who emphasized that lower Carr's index values correlate with improved flowability and processing efficiency in pharmaceutical manufacturing. In our study, the Carr's index of nanoballoons demonstrated superior flowability compared to ibuprofen, suggesting that these nanoballoons may enhance the manufacturability of drug formulations. This is consistent with the results reported by Serrano-Mora *et al.* (2021),²⁹ where their co-processed excipients exhibited Carr's index values ranging from 16% to 20%, indicating less favorable flow properties compared to our findings. The findings from our research, indicating that the Carr's index of

nanoballoons is lower than that of ibuprofen, suggest that these nanoballoons could potentially facilitate more efficient manufacturing processes. This aligns with broader trends observed in the pharmaceutical industry regarding the development of advanced excipients and drug delivery systems.³⁰

The Hausner ratio for nanoballoons indicated good flow properties. Recent studies have established that Hausner ratios below 1.25–1.30 are optimal for ensuring good flowability in pharmaceutical formulations.^{31,32} This aligns with the findings of Monton *et al.*, who emphasized that the Hausner ratio, along with other parameters such as the Carr index, is integral to assessing the flow properties of drug powders.³³

Perhaps most significantly, the angle of repose for nanoballoons demonstrated excellent flow characteristics, substantially better than ibuprofen. A recent study noted that optimal processing conditions are typically associated with angles below 30°.³⁴ This observation is further supported by the work of Azman *et al.* (2021),³⁵ who highlighted that angles of repose are influenced by moisture content, which can affect material flow characteristics. The practical implications of a lower angle of repose are substantial for manufacturing. Materials with a lower angle of repose tend to be more flowable, facilitating easier handling and processing. For instance, Azman *et al.* emphasized that the angle of repose is essential for the design of processing, storage, and conveying systems for particulate materials.

Buoyancy study

The buoyancy studies revealed good floating capabilities of the ibuprofen nanoballoons, with 93.5% of the formulation maintaining buoyancy over 12 h. This performance aligns with recent advances in floating drug delivery systems, where optimization of floating parameters is critical for sustained gastric retention.³⁶ The immediate onset of floating behavior without lag time can be attributed to the optimized hollow core structure, corroborated by the low bulk density, consistent with recent findings.³⁷ The hollow architecture's contribution to floating behavior can be explained by the ethyl cellulose matrix providing mechanical stability while maintaining low density.³⁸ Further, SEM analysis confirmed uniform wall thickness and structural consistency. This observation aligns with the recent findings by Raje *et al.* (2022),³⁹ emphasizing that wall thickness can be manipulated to control drug release profiles, linking structural parameters to functional outcomes in drug delivery systems. Additionally, Kulkarni *et al.* (2022)⁴⁰ highlighted that microstructural properties, including wall thickness, significantly influence the drug release mechanisms in formulations, reinforcing the importance of uniformity in achieving desired therapeutic effects.

The porous surface morphology further enhances floating capability due to additional air pockets, contributing to the overall buoyancy. The incorporation of porous structures not only facilitates the retention of air but also increases the surface area for drug release, leading to a controlled and sustained release profile.⁴¹ The observed 63% reduction in bulk density relative to ibuprofen significantly exceeds the critical threshold of 50% for optimal gastric retention established by Dhukia *et al.* (2024).⁴² This reduction indicates a favorable alteration in the formulation that enhances buoyancy and prolongs gastric retention time, which is essential for improving the bioavailability of poorly soluble drugs like ibuprofen.⁴³ The relationship between bulk density and gastric retention is well-documented; lower bulk density formulations tend to remain in the stomach longer, facilitating sustained drug release and absorption.^{44,45}

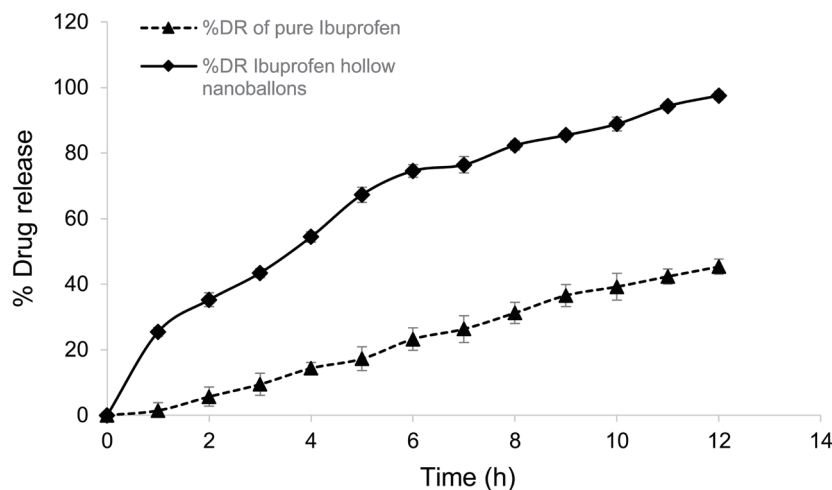


Fig. 3. Drug release profiles of ibuprofen and ibuprofen nanoballoons.

Morphological characteristics of the ibuprofen-loaded floating nanoballoons examined using SEM

The SEM micrographs revealed that the nanoballoons exhibited a spherical morphology with a distinct hollow core structure (Fig. 2). The spherical morphology and well-defined boundaries of the nanoballoons are critical for maintaining structural integrity in the harsh gastric environment, which is essential for gastroretentive applications.⁴⁶ The nanoballoons displayed a porous surface topology, which is advantageous for enhancing drug dissolution and release.⁴⁷ The increased surface area associated with porous structures facilitates a higher drug loading capacity and promotes rapid diffusion of the drug molecules into the surrounding medium, thereby accelerating the release rate.⁴⁸

In vitro drug release

The observed biphasic drug release profile of ibuprofen-loaded floating nanoballoons (Fig. 3) is indicative of a well-designed delivery system that can provide both immediate and prolonged therapeutic effects. The initial burst release of 35.23% within the first two hours aligns with findings from other studies that highlight the significance of initial rapid drug release in enhancing therapeutic efficacy while minimizing dosing frequency.⁴⁹ The initial burst release can be attributed to the surface-adsorbed drug molecules and the presence of the microporous surface architecture, which facilitates rapid drug dissolution for immediate therapeutic onset. The sustained release phase, which culminates in 97.54% release over 12 h, supports the notion that floating systems can improve drug bioavailability by maintaining drug concentration in the gastric environment.⁵⁰

The Korsmeyer-Peppas model fitting with an exponent ($n = 0.4327$) suggests an anomalous transport mechanism, which is consistent with literature indicating that such mechanisms often involve a combination of Fickian diffusion and polymer relaxation.⁵¹ This dual mechanism is crucial for achieving a controlled release profile, as it allows for the modulation of drug release rates based on the formulation's physicochemical properties.⁵² Statistical validation through one-way ANOVA confirms the robustness of the release data, reinforcing the potential of these nanoballoons in clinical applications aimed at improving patient compliance and therapeutic outcomes.⁵³

The complex release mechanism elucidated by our kinetic analysis has important implications for the therapeutic efficacy of the

ibuprofen nanoballoons. The initial burst release provides a rapid onset of action, which is beneficial for achieving quick pain relief. The subsequent sustained release, governed by anomalous transport, ensures a prolonged therapeutic effect, potentially reducing dosing frequency and improving patient compliance. Moreover, the combination of diffusion and erosion-controlled release suggests that the nanoballoons may provide a more consistent drug release rate over time compared to purely diffusion-controlled systems. This could lead to more stable plasma concentrations of ibuprofen, potentially enhancing its anti-inflammatory and analgesic effects while minimizing fluctuations that could lead to side effects.

Animal model, grouping, and treatments

In this study, male Sprague-Dawley rats were utilized to evaluate the anti-inflammatory effects of ibuprofen nanoballoons. The acute anti-inflammatory model demonstrated that the group receiving ibuprofen nanoballoons exhibited a statistically significant reduction in paw edema compared to both the control and pure ibuprofen groups at all measured time points, with a peak percentage inhibition of 68.12% at the third hour post-injection.⁵⁴ In the chronic model, the nanoballoons group also showed significant reductions in inflammatory markers such as TNF- α , hs-CRP, and IL-6, while increasing IL-10 levels, indicating a favorable modulation of the inflammatory response.⁵⁵ These findings suggest that the nanoballoon formulation enhances the bioavailability and therapeutic efficacy of ibuprofen, highlighting the potential of nanotechnology in improving anti-inflammatory treatments.⁵⁶

Limitations of the study

While our study demonstrates promising results for ibuprofen-loaded floating nanoballoons, several limitations should be acknowledged. The *in vivo* studies, although comprehensive, were conducted solely in rodent models, and human clinical trials are needed to validate these findings. Long-term stability studies under various storage conditions would also be valuable. Our investigation focused primarily on anti-inflammatory effects, leaving other potential therapeutic benefits unexplored. The manufacturing process, while successful at the laboratory scale, requires further optimization for industrial-scale production. Additionally, we did not investigate the potential impact of food intake on the gastric retention time of the

nanoballoons, which could affect their clinical performance. A cost-effectiveness analysis and comparison with existing commercial formulations were beyond the scope of this study. Understanding these limitations provides direction for future research to enhance the clinical applicability of this novel drug delivery system.

Future research directions

The successful development of ibuprofen-loaded floating nanoballoons opens several promising avenues for future research and therapeutic applications. We hypothesize that the nanoballoon delivery system can be further optimized through surface modification techniques to enhance mucoadhesion properties, potentially extending gastric retention time beyond current capabilities. Future studies should focus on comparative pharmacokinetics through head-to-head comparisons with commercial sustained-release formulations, investigation of bioavailability enhancement mechanisms, and population pharmacokinetic modeling for dose optimization. Advanced formulation strategies will explore the integration of smart polymers responsive to inflammatory markers, the development of dual-drug-loaded nanoballoons for synergistic effects, and alternative biodegradable polymers for enhanced sustainability. Clinical translation will require long-term stability studies, scale-up process optimization, and cost-effectiveness analysis. The therapeutic potential can be expanded through the application to other poorly water-soluble drugs, investigation of chronic disease management applications, and development of patient-specific formulation parameters. We anticipate that these research directions will lead to the development of more efficient drug delivery systems with improved therapeutic outcomes and patient compliance. The potential for personalized medicine approaches using nanoballoon technology could revolutionize the treatment of chronic inflammatory conditions.

Conclusions

The study successfully developed and characterized floating nanoballoons of ibuprofen using the solvent evaporation technique, demonstrating a promising gastro-retentive drug delivery system. The nanoballoons exhibited favorable micromeritic properties, excellent buoyancy, and a biphasic drug release profile, with an initial burst followed by sustained release over 12 h. The spherical morphology and porous structure of the nanoballoons contributed to their enhanced floatability and sustained drug release. These findings suggest that floating nanoballoons can significantly improve the bioavailability of poorly water-soluble drugs like ibuprofen by prolonging gastric residence time and minimizing drug degradation in acidic environments. Further optimization of production processes and stability testing may enhance this formulation's clinical application, potentially reducing dosing frequency and improving patient compliance. This innovative delivery system holds great promise for addressing the limitations associated with conventional oral administration of ibuprofen.

Acknowledgments

None.

Funding

None.

Conflict of interest

The authors declare that they have no known competing financial interests or personal relationships that could have appeared to influence the work reported in this paper.

Author contributions

Involved in conceptualizing, design, drafting, and critical revision of the manuscript (AKP, BAS), Involved in in-vivo work (BAM), statistical analysis (BAM), involved in data analysis (HAA), Drafting the manuscript (HAA). All authors have read and approved the final version.

Ethical statement

The protocol was approved by the Committee on the Ethics of Animal Experiments of the University of Al Qadisiyah (Protocol Number: 84). All surgery was performed under ketamine/xylazine anesthesia, and all efforts were made to minimize suffering.

Data sharing statement

The datasets used in support of the findings of this study have not been made available because of intellectual property protection and ongoing research developments.

References

- [1] Homayun B, Lin X, Choi HJ. Challenges and Recent Progress in Oral Drug Delivery Systems for Biopharmaceuticals. *Pharmaceutics* 2019;11(3):129. doi:10.3390/pharmaceutics11030129, PMID:30893852.
- [2] Yashavanth G, Prakash SG, Mallamma T. Floating drug delivery system: A review. *Int J Adv Res* 2022;10:161–167. doi:10.21474/IJAR01/15653.
- [3] Alqahtani MS, Kazi M, Alsenaidy MA, Ahmad MZ. Advances in Oral Drug Delivery. *Front Pharmacol* 2021;12:618411. doi:10.3389/fphar.2021.618411, PMID:33679401.
- [4] Çalışıcı D, Yılmaz S, Goktas B. Toxic, Genotoxic and Teratogenic Effects of Ibuprofen and its Derivatives. *Curr Drug Targets* 2023;24(4):361–370. doi:10.2174/1389450124666230104160435, PMID:36600619.
- [5] Zappaterra F, Rodriguez MEM, Summa D, Semeraro B, Costa S, Tamburini E. Biocatalytic Approach for Direct Esterification of Ibuprofen with Sorbitol in Biphasic Media. *Int J Mol Sci* 2021;22(6):3066. doi:10.3390/ijms22063066, PMID:33802769.
- [6] Shamsian S, Sokouti B, Dastmalchi S. Benchmarking different docking protocols for predicting the binding poses of ligands complexed with cyclooxygenase enzymes and screening chemical libraries. *Bioimpacts* 2024;14(2):29955. doi:10.34172/bi.2023.29955, PMID:38505677.
- [7] Irvine J, Afrose A, Islam N. Formulation and delivery strategies of ibuprofen: challenges and opportunities. *Drug Dev Ind Pharm* 2018;44(2):173–183. doi:10.1080/03639045.2017.1391838, PMID:2902772.
- [8] Hawlitschek C, Brendel J, Gabriel P, Schierle K, Salameh A, Zimmer HG, *et al*. How Effective Is a Late-Onset Antihypertensive Treatment? Studies with Captopril as Monotherapy and in Combination with Nifedipine in Old Spontaneously Hypertensive Rats. *Biomedicines* 2022;10(8):1964. doi:10.3390/biomedicines10081964, PMID:36009511.
- [9] Weiser T, Schepers C, Mück T, Lange R. Pharmacokinetic Properties of Ibuprofen (IBU) From the Fixed-Dose Combination IBU/Caffeine (400/100 mg; FDC) in Comparison With 400 mg IBU as Acid or Lysinate Under Fasted and Fed Conditions-Data From 2 Single-Center, Single-Dose, Randomized Crossover Studies in Healthy Volunteers. *Clin Pharmacol Drug Dev* 2019;8(6):742–753. doi:10.1002/cpdd.672,

- PMID:30897305.
- [10] Hens B, Tsume Y, Bermejo M, Paixao P, Koenigsnecht MJ, Baker JR, *et al*. Low Buffer Capacity and Alternating Motility along the Human Gastrointestinal Tract: Implications for in Vivo Dissolution and Absorption of Ionizable Drugs. *Mol Pharm* 2017;14(12):4281–4294. doi:10.1021/acs.molpharmaceut.7b00426, PMID:28737409.
 - [11] Koenigsnecht MJ, Baker JR, Wen B, Frances A, Zhang H, Yu A, *et al*. In Vivo Dissolution and Systemic Absorption of Immediate Release Ibuprofen in Human Gastrointestinal Tract under Fed and Fasted Conditions. *Mol Pharm* 2017;14(12):4295–4304. doi:10.1021/acs.molpharmaceut.7b00425, PMID:28937221.
 - [12] Komori K, Fukuda M, Matsuura T, Yamada S, Mitamura S, Konishi R, *et al*. Effect of alcoholic beverages on drug absorption: blood concentration profile of ibuprofen in mice. *J Appl Pharm* 2017;9(2):1000237. doi:10.21065/1920-4159.1000237.
 - [13] Shin D, Lee SJ, Ha YM, Choi YS, Kim JW, Park SR, *et al*. Pharmacokinetic and pharmacodynamic evaluation according to absorption differences in three formulations of ibuprofen. *Drug Des Devel Ther* 2017;11:135–141. doi:10.2147/DDDT.S121633, PMID:28115830.
 - [14] Abdalkader H, Abdel-Aleem JA, Mousa HS, Elgendy MO, Al Fatease A, Abou-Taleb HA. Captopril Polyvinyl Alcohol/Sodium Alginate/Gelatin-Based Oral Dispersible Films (ODFs) with Modified Release and Advanced Oral Bioavailability for the Treatment of Pediatric Hypertension. *Pharmaceuticals (Basel)* 2023;16(9):1323. doi:10.3390/ph16091323, PMID:37765131.
 - [15] Das U, Wadhwa P, Singh PK, Kalidindi DV, Nagpal K. The Role of Polymers and Excipients for Better Gastric Retention of Captopril. *Crit Rev Ther Drug Carrier Syst* 2022;39(6):85–106. doi:10.1615/CritRevTherDrugCarrierSyst.2022042122, PMID:35997102.
 - [16] Ryu GY, Jae H, Kim K, Kim H, Lee S, Jeon Y, *et al*. Hollow heteropoly acid-functionalized zif composite membrane for proton exchange membrane fuel cells. *ACS Appl Energy Mat* 2023;6(8):4283–4296. doi:10.1021/acsaem.3c00220.
 - [17] Ghoneim AM, Tadros MI, Alaa-Eldin AA. Spray-Dried Silica Xerogel Nanoparticles as a Promising Gastroretentive Carrier System for the Management of Chemotherapy-Induced Nausea and Vomiting. *Int J Nanomedicine* 2019;14:9619–9630. doi:10.2147/IJN.S232841, PMID:31824155.
 - [18] Ahmad S, Khan JA, Kausar TN, Mahnashi MH, Alasiri A, Alqahtani AA, *et al*. Preparation, Characterization and Evaluation of Flavonolignan Silymarin Effervescent Floating Matrix Tablets for Enhanced Oral Bioavailability. *Molecules* 2023;28(6):2606. doi:10.3390/molecules28062606, PMID:36985575.
 - [19] Jeong HM, Weon KY, Shin BS, Shin S. 3D-Printed Gastroretentive Sustained Release Drug Delivery System by Applying Design of Experiment Approach. *Molecules* 2020;25(10):2330. doi:10.3390/molecules25102330, PMID:32429452.
 - [20] Rohilla S, Bhatt D, Ahalwat S. Fabrication of potential gastroretentive microspheres of itraconazole for stomach-specific delivery: Statistical optimization and in vitro evaluation. *J Appl Pharm Sci* 2020;10(3):119–127. doi:10.7324/japs.2020.103016.
 - [21] Fu K, Zhou Y, Hou J, Shi T, Ni J, Li X, *et al*. Floating poly(lactic-co-glycolic acid)-based controlled-release drug delivery system for intravesical instillation. *J Int Med Res* 2023;51(4):3000605231162065. doi:10.1177/03000605231162065, PMID:37038914.
 - [22] Dos Santos-Silva AM, de Caland LB, do Nascimento EG, Oliveira ALCSL, de Araújo-Júnior RF, Cornélio AM, *et al*. Self-Assembled Benzimidazole-Loaded Cationic Nanoparticles Containing Cholesterol/Sialic Acid: Physicochemical Properties, In Vitro Drug Release and In Vitro Anticancer Efficacy. *Int J Mol Sci* 2019;20(9):2350. doi:10.3390/ijms20092350, PMID:31083590.
 - [23] Lee K, Khan F, Cosby L, Yang G, Winter J. Polymer concentration maximizes encapsulation efficiency in electrohydrodynamic mixing nanoprecipitation. *Front. Nanotechnol* 2021;3:1–14. doi:10.3389/fnano.2021.719710.
 - [24] Tan SP, Kha TC, Parks S, Stathopoulos C, Roach PD. Optimising the Encapsulation of an Aqueous Bitter Melon Extract by Spray-Drying. *Foods* 2015;4(3):400–419. doi:10.3390/foods4030400, PMID:28231214.
 - [25] Mintis DG, Dompé M, Kamperman M, Mavrantzas VG. Effect of Polymer Concentration on the Structure and Dynamics of Short Poly(N,N-dimethylaminoethyl methacrylate) in Aqueous Solution: A Combined Experimental and Molecular Dynamics Study. *J Phys Chem B* 2020;124(1):240–252. doi:10.1021/acs.jpcc.9b08966, PMID:31820991.
 - [26] Bagde S, Gupta DK, Manglawat SK, Choukse R, Patel R. Formulation, optimization and evaluation of floating nanoballoons of ibuprofen. *Asian J Biomed Pharm Sci* 2012;2:1–10. doi:10.20959/wjpps.20195-13616.
 - [27] Makovníková J, Širáň M, Houšková B, Pálka B, Jones A. Comparison of different models for predicting soil bulk density. case study – slovakian agricultural soils. *Int Agrophys* 2017;31(4):491–498. doi:10.1515/intag-2016-0079.
 - [28] Gashe F, Assefa D, Tesema S, Zeleke G, Tatiparthi R, Kebebe D, *et al*. Characterization of *Boswellia rivae* Engl Resin as a Potential Use for Pharmaceutical Excipient. *Biomed Res Int* 2022;2022:5791308. doi:10.1155/2022/5791308, PMID:35978631.
 - [29] Serrano-Mora LE, Zambrano-Zaragoza ML, Mendoza-Muñoz N, Leyva-Gómez G, Urbán-Morlán Z, Quintanar-Guerrero D. Preparation of Co-Processed Excipients for Controlled-Release of Drugs Assembled with Solid Lipid Nanoparticles and Direct Compression Materials. *Molecules* 2021;26(7):2093. doi:10.3390/molecules26072093, PMID:33917445.
 - [30] Diaz L, Brown C, Ojo E, Mustoe C, Florence A. Machine learning approaches to the prediction of powder flow behaviour of pharmaceutical materials from physical properties. *Digit Discover* 2023;2(3):692–701. doi:10.1039/d2dd00106c.
 - [31] Marinucci F, Aversa A, Manfredi D, Lombardi M, Fino P. Evaluation of a Laboratory-Scale Gas-Atomized AlSi10Mg Powder and a Commercial-Grade Counterpart for Laser Powder Bed Fusion Processing. *Materials (Basel)* 2022;15(21):7565. doi:10.3390/ma15217565, PMID:36363164.
 - [32] Khadivi A, Mirheidari F, Saeidifari A, Moradi Y. Selection of the promising accessions of jamun (*Syzygium cumini* (L.) skeels) based on pomological characterizations. *Food Sci Nutr* 2023;11(1):470–480. doi:10.1002/fsn3.3078, PMID:36655090.
 - [33] Monton C, Sangprapai T, Mekwimonmas N, Sawangsang T, Chankana N, Luprasong C. Application of simplex lattice design in formulation development of lozenges containing *vernonia cinerea* extract for smoking cessation. *Key Engineering Materials* 2019;819:227–232. doi:10.4028/www.scientific.net/kem.819.227.
 - [34] Shah DS, Moravkar KK, Jha DK, Lonkar V, Amin PD, Chalikwar SS. A concise summary of powder processing methodologies for flow enhancement. *Heliyon* 2023;9(6):e16498. doi:10.1016/j.heliyon.2023.e16498, PMID:37292344.
 - [35] Azman WMFBW, Shamsudin R, Nor MYM, Hamzah A. Effect of moisture content on the angle of repose and coefficient of kinetic friction of sago trunk (*metroxylo* spp.). *Adv Agri Food Res J* 2021;2(1):a0000179. doi:10.36877/aafrj.a0000179.
 - [36] Liang YK, Cheng WT, Chen LC, Sheu MT, Lin HL. Development of a Swellable and Floating Gastroretentive Drug Delivery System (sfGRDDS) of Ciprofloxacin Hydrochloride. *Pharmaceutics* 2023;15(5):1428. doi:10.3390/pharmaceutics15051428, PMID:37242670.
 - [37] Souza MPC, Sábio RM, Ribeiro TC, Santos AMD, Meneguín AB, Chorilli M. Highlighting the impact of chitosan on the development of gastroretentive drug delivery systems. *Int J Biol Macromol* 2020;159:804–822. doi:10.1016/j.ijbiomac.2020.05.104, PMID:32425271.
 - [38] Sharma M, Kohli S, Dinda A. In-vitro and in-vivo evaluation of repaglinide loaded floating microspheres prepared from different viscosity grades of HPMC polymer. *Saudi Pharm J* 2015;23(6):675–682. doi:10.1016/j.jsps.2015.02.013, PMID:26702263.
 - [39] Rajee V, Palekar S, Banella S, Patel K. Tunable Drug Release from Fused Deposition Modelling (FDM) 3D-Printed Tablets Fabricated Using a Novel Extrudable Polymer. *Pharmaceutics* 2022;14(10):2192. doi:10.3390/pharmaceutics14102192, PMID:36297626.
 - [40] Kulkarni VR, Kazi M, Shahba AA, Radhanpuri A, Maniruzzaman M. Three-Dimensional Printing of a Container Tablet: A New Paradigm for Multi-Drug-Containing Bioactive Self-Nanoemulsifying Drug-Delivery Systems (Bio-SNEDDSs). *Pharmaceutics* 2022;14(5):1082. doi:10.3390/pharmaceutics14051082, PMID:35631668.
 - [41] Bakre LG, Ladele BA. Development and evaluation of gastroretentive ciprofloxacin floating tablets using *chrysophyllum albidum* gum. *J*

- Pharm Pract Res 2019;49(3):240–245. doi:10.1002/jppr.1503.
- [42] Dhukia S, Chanu AR, Sagar S, Jaleel J, Gupta P, Khan D, *et al*. Normative Data of Liquid Gastric Emptying and Small-bowel Transit: A Prospective Cross-sectional Study. *Indian J Nucl Med* 2024;39(2):98–105. doi:10.4103/ijnm.ijnm_148_23, PMID:38989310.
- [43] Katona MT, Nagy-Katona L, Szabó R, Borbás E, Tonka-Nagy P, Takács-Novák K. Multi-Compartmental Dissolution Method, an Efficient Tool for the Development of Enhanced Bioavailability Formulations Containing Poorly Soluble Acidic Drugs. *Pharmaceutics* 2023;15(3):753. doi:10.3390/pharmaceutics15030753, PMID:36986614.
- [44] Reddy PS, Alagarsamy V, Chandra Bose PS. Formulation and In-vitro evaluation of amlodipine besylate floating tablets using different polymers. *Int J Res Rev* 2023;10(9):500–510. doi:10.52403/ijrr.20230951.
- [45] Bonsode DA. Advances in the preparation techniques of floating microspheres with exploration of ai tool in product development. *Pharma Drug Reg Affairs J* 2023;6(1):1–17. doi:10.23880/pdraj-16000146.
- [46] Gao Y, Bai Y, Zhao D, Chang MW, Ahmad Z, Li JS. Tuning microparticle porosity during single needle electrospraying synthesis via a non-solvent-based physicochemical approach. *Polymers* 2015;7(12):2701–2710. doi:10.3390/polym7121531.
- [47] Sun B, Yeo Y. Nanocrystals for the parenteral delivery of poorly water-soluble drugs. *Curr Opin Solid State Mater Sci* 2012;16(6):295–301. doi:10.1016/j.cossms.2012.10.004, PMID:23645994.
- [48] Asikainen S, Bochove BV, Seppälä J. Drug-releasing biopolymeric structures manufactured via stereolithography. *Biomed Phys Engg Exp* 2019;5(2):025008. doi:10.1088/2057-1976/aaf0e0.
- [49] Oh SJ, Jung JH. Sustainable Drug Release Using Nanoparticle Encapsulated Microneedles. *Chem Asian J* 2022;17(16):e202200333. doi:10.1002/asia.202200333, PMID:35644865.
- [50] Bakre LG, Ladele BA. Development and evaluation of gastroretentive ciprofloxacin floating tablets using chrysophyllum albidum gum. *J Pharm Pract Res* 2019;49(3):240–245. doi:10.1002/jppr.1503.
- [51] Noureen S, Noreen S, Ghumman SA, Batool F, Hameed H, Hasan S, *et al*. Prunus armeniaca Gum-Alginate Polymeric Microspheres to Enhance the Bioavailability of Tramadol Hydrochloride: Formulation and Evaluation. *Pharmaceutics* 2022;14(5):916. doi:10.3390/pharmaceutics14050916, PMID:35631501.
- [52] Li T, Chan JW, Uhrich KE. Drug loading and release kinetics in polymeric micelles: comparing dynamic versus unimolecular sugar-based micelles for controlled release. *J Bioact Compat Polym* 2015;31(3):227–241. doi:10.1177/0883911515609814.
- [53] Adeleke OA, Choonara YE, Du Toit LC, Pillay V. In vivo and ex vivo evaluation of a multi-particulate composite construct for sustained transbuccal delivery of carbamazepine. *J Pharm Sci* 2014;103(4):1157–1169. doi:10.1002/jps.23884, PMID:24765650.
- [54] Liu S, Hu C, Li F, Li XJ, Cui W, Fan C. Prevention of peritendinous adhesions with electrospun ibuprofen-loaded poly(L-lactic acid)-polyethylene glycol fibrous membranes. *Tissue Eng Part A* 2013;19(3-4):529–537. doi:10.1089/ten.TEA.2012.0208, PMID:23013368.
- [55] De Logu F, Li Puma S, Landini L, Tuccinardi T, Poli G, Preti D, *et al*. The acyl-glucuronide metabolite of ibuprofen has analgesic and anti-inflammatory effects via the TRPA1 channel. *Pharmacol Res* 2019;142:127–139. doi:10.1016/j.phrs.2019.02.019, PMID:30794923.
- [56] Warmink K, Rios JL, van Valkengoed DR, Korthagen NM, Weinans H. Sprague Dawley Rats Show More Severe Bone Loss, Osteophytosis and Inflammation Compared to Wistar Han Rats in a High-Fat, High-Sucrose Diet Model of Joint Damage. *Int J Mol Sci* 2022;23(7):3725. doi:10.3390/ijms23073725, PMID:35409085.